Electron-Induced Decomposition of V_2MoO_8 and $(V_{0.7}Mo_{0.3})_2O_5$ during Imaging in the Electron Microscope

Z. C. KANG AND L. EYRING

*Department of Chemistry and the Center for Solid State Science,
Arizona State University, Tempe, Arizona 85287*

The two compounds V_2MoO_8 and $(V_{0.7}Mo_{0.3})_2O_5$ are observed to decompose *in situ* in the electron microscope during HRTEM observation at near atomic resolution. Oriented VO is the identifiable final product in each decomposition. There is a different unidentified intermediate to the decomposition for each compound. $(V_{0.7}Mo_{0.3})_2O_5$ is not an intermediate of the decomposition of V_2MoO_8. Aside from gaining information on these specific decompositions, these studies broaden our insight into *in-situ* reactions that occur during HRTEM observations. © 1992 Academic Press, Inc.

Introduction

High-resolution electron microscopy possesses the capability to follow solid-state chemical reactions at essentially the atomic level *in situ* during observation. It is important to gain experience in such studies that can help distinguish the special electron beam effects beyond those undifferentiated energy absorption events that give results similar to ordinary heating. This experience can most effectively be gained when reactions that have been thoroughly investigated outside the microscope are studied *in situ* within the microscope. In many cases electron beam irradiation results in reactions that would not occur in the vacuum of the specimen chamber at any temperature reasonably caused by the beam required for observation. There are examples where oxidation, reduction, synthesis, or decomposition have occurred during microscopal observation that could not occur without some direct effect of the electron irradiation. In this study a system capable of exhibiting either oxidation or reduction is examined using HREM techniques and analysis.

Previous studies (*1*) have suggested that the reaction

$$10(V_{0.7}Mo_{0.3})_2O_5) + \tfrac{3}{2}O_2 \rightarrow 6V_2MoO_8 + V_2O_5$$
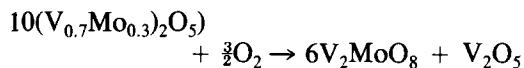
can be reversed at 450–650°C at a sufficiently low oxygen activity. This solid-state reaction requires the loss of oxygen as well as the transport of vanadium to form the final single phase. At appropriate oxygen partial pressures, only the molybdenum is reduced, and this to the plus-five state. In oxidation in the same temperature range, both the vanadium and molybdenum are brought to their maximal valence state, plus-five and plus-six, respectively, requiring the unmixing of the metal atoms since
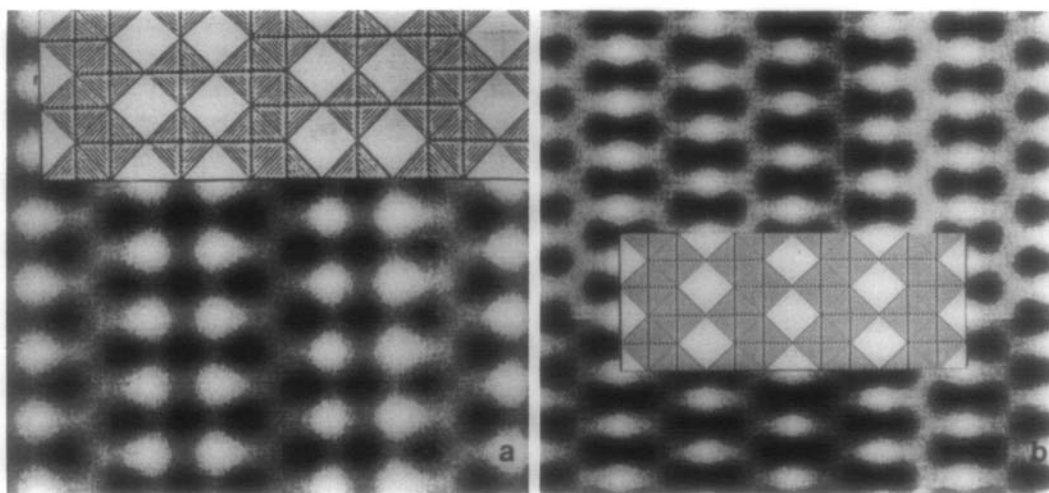
FIG. 1. The projection of the known structure and the calculated image in the [0 0 1] directions of (a) V_2MoO_8 and (b) $(V_{0.7}Mo_{0.3})_2O_5$.

there would then be an excess of vanadium.

Subsequently Kang *et al.* (2) made observations during an electron microscope study that differed from the equilibrium investigation referred to above in some respects. A principle discrepancy was that all the V_2O_5-type structures observed were shown, by EDX measurements, to be ternary phases containing up to about 0.2 atom fraction isomorphous replacement of vanadium by Mo as $(V_xMo_{(1-x)})_2O_5$. These latter authors also suggested the mechanism of the oxidation–reduction reaction from the HREM observations.

If these vanadium–molybdenum oxide specimens are observed over tens of minutes a new structure is observed progressively to appear, primarily from the thinner parts of the crystal. The purpose here is to explore these additional observations in the light of previous work.

Experimental

The specimens of V_2MoO_8 and $(Mo_{0.3}V_{0.7})_2O_5$ were prepared as previously described (1). Samplings of each preparation were applied to holey carbon grids from ethanol suspensions. HREM observations were made using a JEOL 4000EX electron microscope equipped with a top-entry specimen holder. During imaging a 120-μm condenser aperture was used along with spot size 3 or 4. This would irradiate the specimen at about 3–5 A/cm² at 500k × magnification.

Calculated Images of the V_2MoO_8 and the $(V_{0.7}Mo_{0.3})_2O_5$ Structures

Eick and Kihlborg (3) and Kihlborg (4) have reported the structures of the original materials. These structures are represented in Figs. 1a,b as projections of atoms and as projections of MO_6 octahedra. The latter representation emphasizes the open tunnels in this [0 0 1] projection. The striking difference between these two structures is the increased edge-sharing in the more reduced material of Fig. 1b. The calculated image is as it should be observed in the microscope for a specimen thickness of 80 Å and at a defocus of −500 Å. The white dots corre-
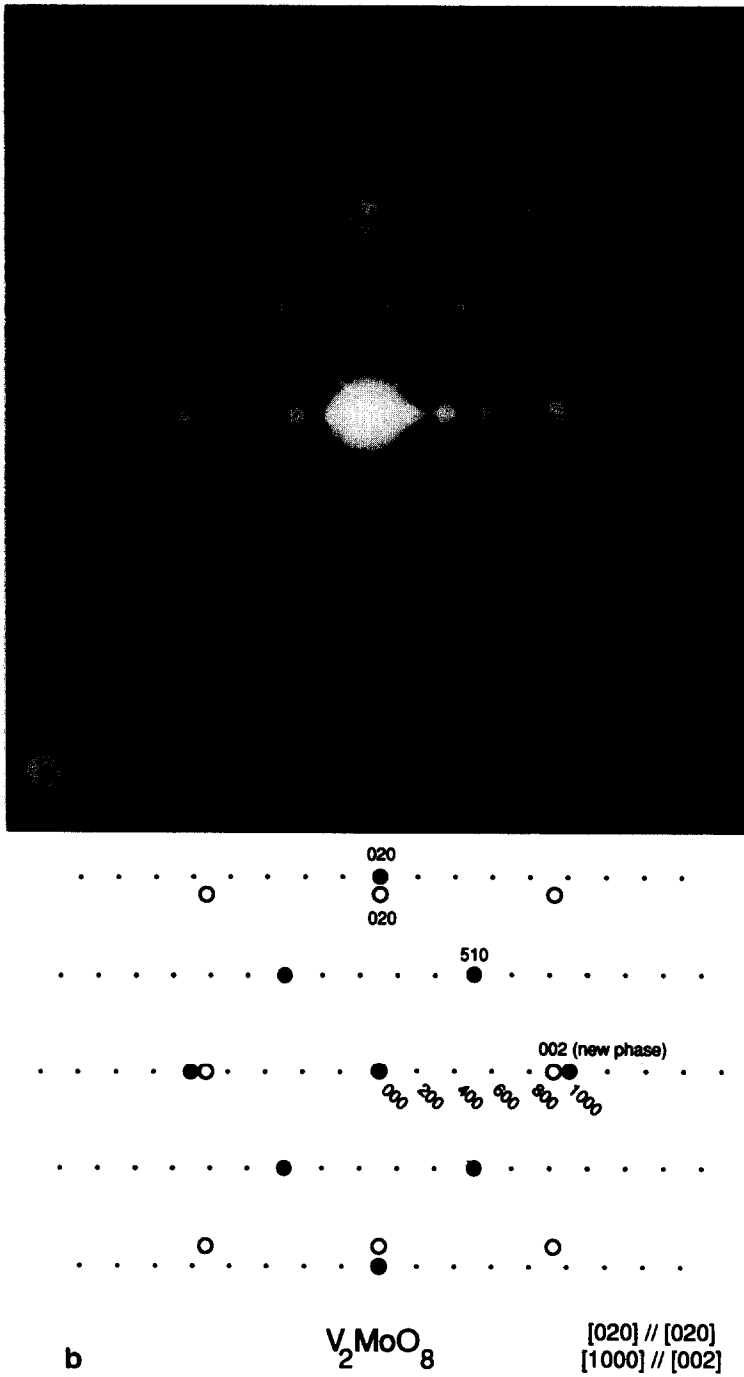
FIG. 2. (a) The diffraction pattern of V_2MoO_8 and its decomposition product. (b) The indexing of the diffraction pattern.

FIG. 3. A high-resolution image of V_2MoO_8 (a) at the beginning of observation. The area A is an undecomposed region. B is a decomposed area. (b) After 20 min exposure to the electron beam.

spond to the tunnels in the structure. These calculated images will serve to identify the starting material and to aid in the interpretation of intergrowth of the new phase that appears as a result of electron beam irradiation.

Decomposition Processes in the V_2MoO_8 Phase

Under settings of the aperture and spot size appropriate to structure imaging, it takes approximately 30 min to decompose
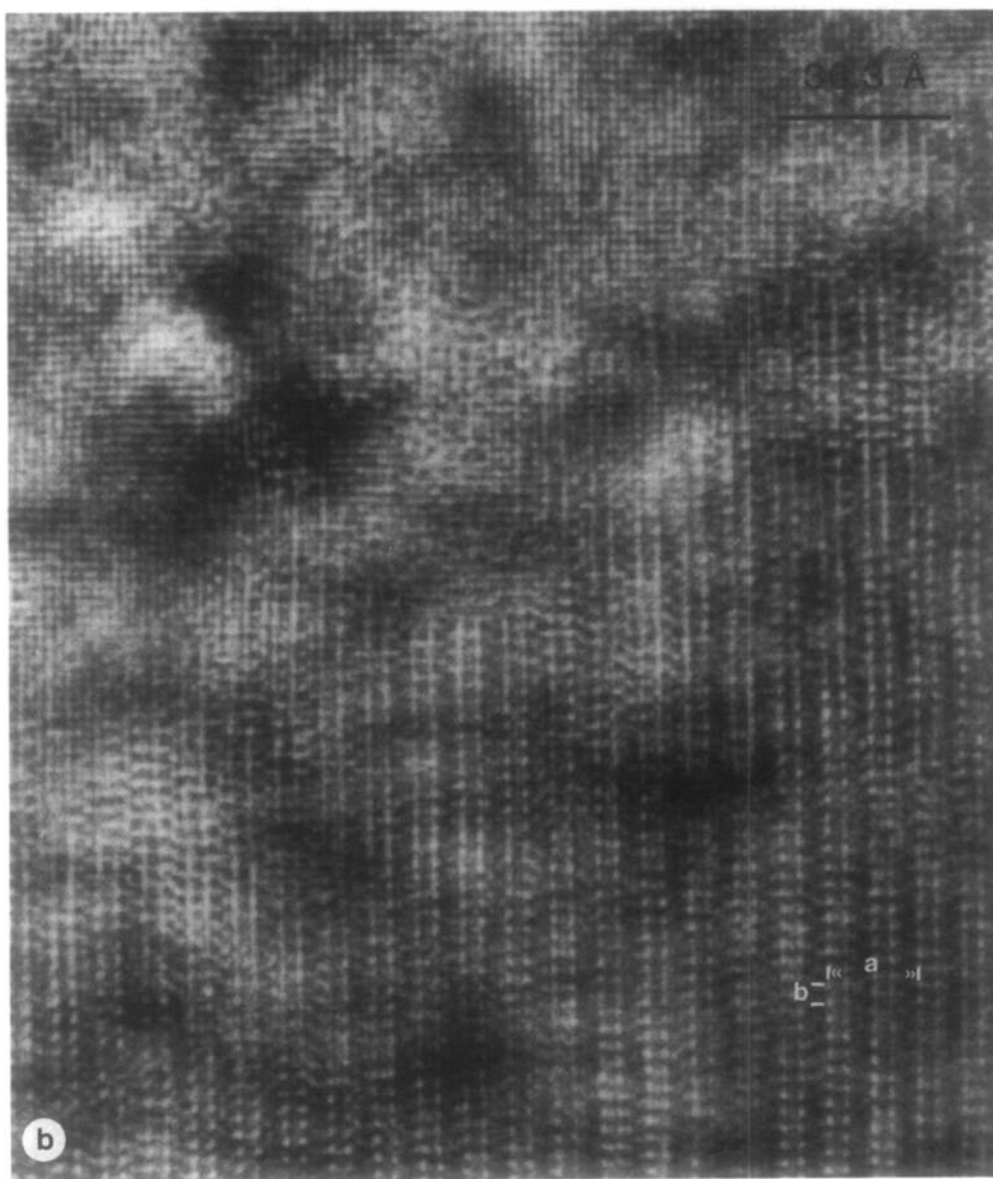
FIG. 3—*Continued*

the specimen to the point that the diffraction spots of the decomposition product appear as a strong and regular pattern as illustrated in Fig. 2a. The diffraction pattern of Fig. 2a is indexed in Fig. 2b to show the relationship between the original and product structures.

The larger solid black spots, two of which are indexed as (10 0 0) and (5 1 0), form a square net that corresponds to the fundamental octahedral network of the original structure. The d-spacings of the two sides of this net are 2.65 and 2.63 Å, respectively,

while that of one diagonal is 1.95 Å. These values are reasonable as the oxygen or metal planar spacing of the coordination octahedra. The spacing of the second diagonal is 1.85 Å, confirming the X-ray result that the metal atom is off-center in the coordination octahedron (3).

The larger square net formed by the open circles represents the product phase with $d_{(1\,0\,0)} = 2.04$ Å. The diagonal of the latter is approximately twice the edge of the net formed by the larger dark spots. It will be useful later if note is taken of the greater spot intensity, in the product structure (Fig. 2a), of those nearest the origin. If the pattern is indexed as f.c.c. as is done in Fig. 2b the cell edge is $a = 4.08$ Å.

Figure 3a shows the experimental high-resolution image of a fragment of V_2MoO_8 at the beginning of observation. The correlation of this image, especially in the lower regions, with that shown calculated in Fig. 1a is obvious. The white dots correlate with the tunnels in the structure. At thinner parts of the crystal, toward the top, changes are clearly underway. There is a band of light contrast near the upper edge caused by the smearing of the original pattern at A in the a direction. The smearing is observed to give way to more closely spaced and more heavily dotted lines at the very edge of the crystal. This development is made clear in the micrograph shown as Fig. 3b taken from the same region, 20 min later. At this later time, the small square net of the product phase is highly developed and its relationship to the original structure is clear. The new net corresponds to the [0 0 1] projection of an f.c.c. structure that could result from the parent structure by a total collapse such that all the octahedra share all edges. In this event the smaller square net formed

would be rotated by 45 degrees, as shown by the diffraction pattern, and the five octahedra across the a direction of the parent unit cell would be replaced by 10 in the same space if it were f.c.c. The white spots could then correspond to the spaces between the columns of metal atoms in the NaCl-type structure (5). If this interpretation is correct there would be a significant decrease in volume leading to a stress that could cause the extremely defective material that results.

Decomposition of the $(V_{0.7}Mo_{0.3})_2O_5$ Phase

The electron-induced decomposition of $(V_{0.7}Mo_{0.3})_2O_5$ proceeds along somewhat dissimilar lines than just described for the oxidized phase, although the final product is the same. Figure 4a exhibits the diffraction pattern of the partially decomposed pentoxide showing, besides the [0 0 1] diffraction pattern of the original material, the diffraction pattern of the same final product, in the same relative orientation, as has just been described. The patterns have been drawn and indexed in Fig. 4b. Again the heavy dark spots correspond to the fundamental octahedral group reflecting a d-spacing of 2.60 Å with a diagonal of 1.93 Å. The weaker intermediate spots arise from the superstructure. The square net of open circles reflects the structure of the product phase with a d-spacing of 2.04 Å and, as before, it is rotated 45 degrees with respect to the orientation of the octahedral subunits. The [0 2 0] of the parent structure is parallel to the [0 2 0] of the product, and the [6 0 0] is parallel to the [0 0 2], respectively. In the diffraction pattern of the final product the extra spots (2 0 0), (4 0 0), etc., have disappeared with the collapse of the octahedral network to form the NaCl-type structure with a loss of oxygen. The image reproduced
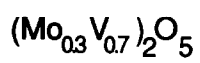

FIG. 4. (a) The diffraction pattern of $(V_{0.7}Mo_{0.3})_2O_5$ and its decomposition product. (b) The indexing of the diffraction pattern.
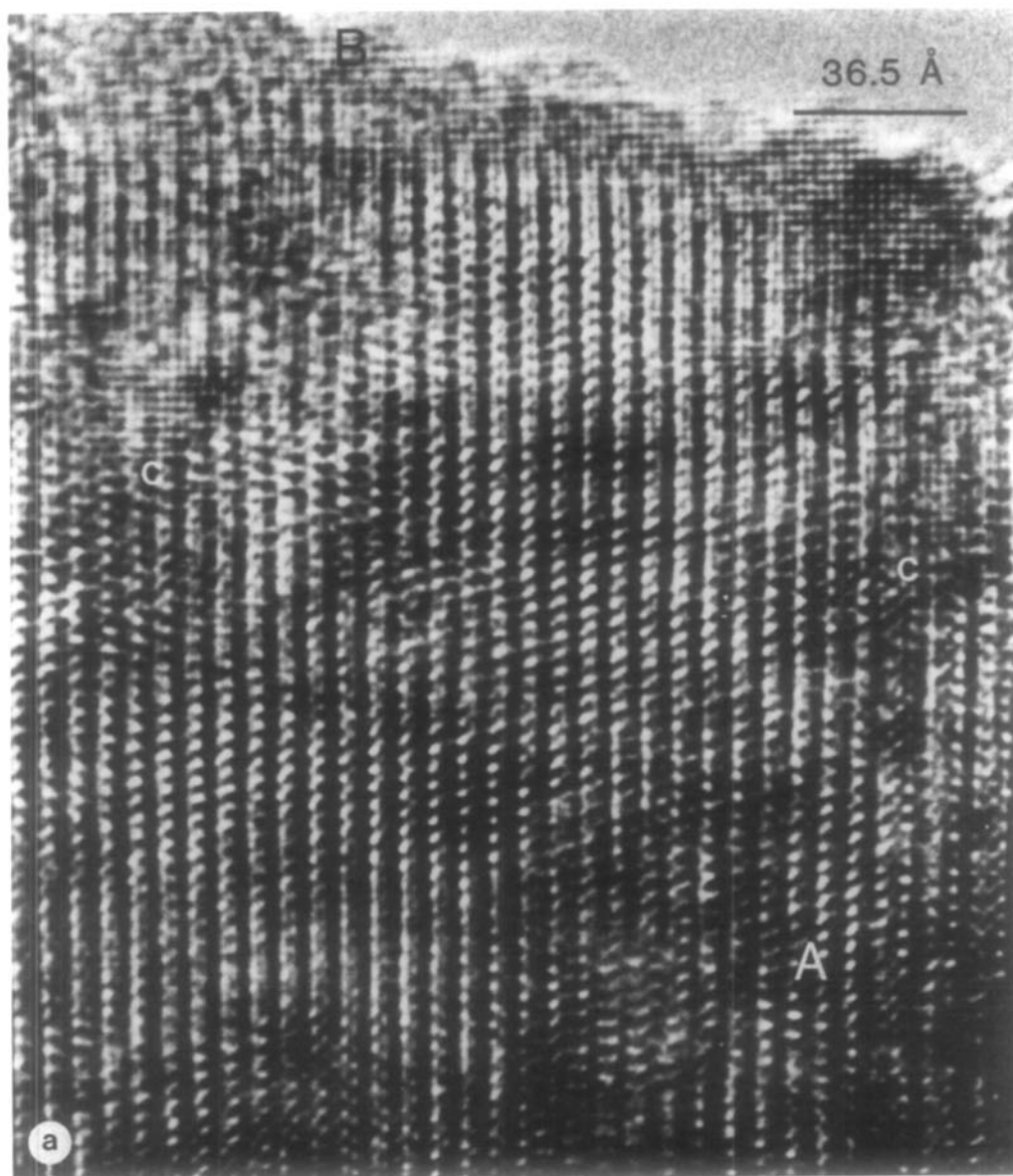
020 // 020
600 // 002

b

$(Mo_{0.3}V_{0.7})_2O_5$
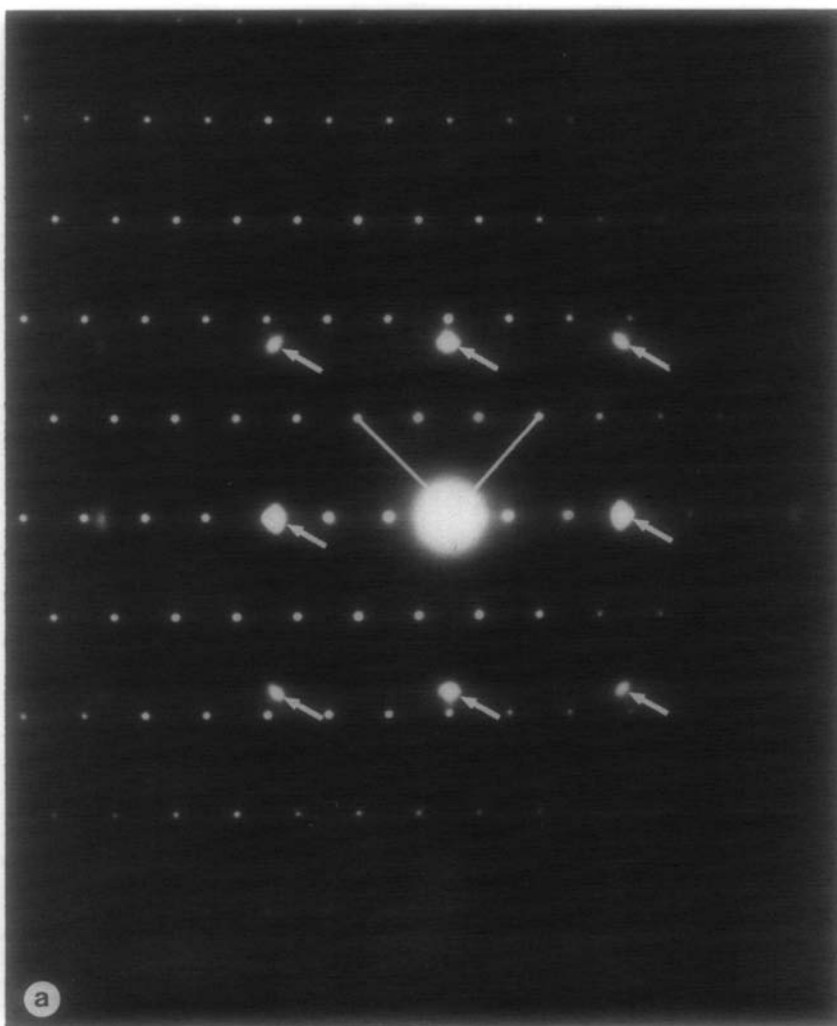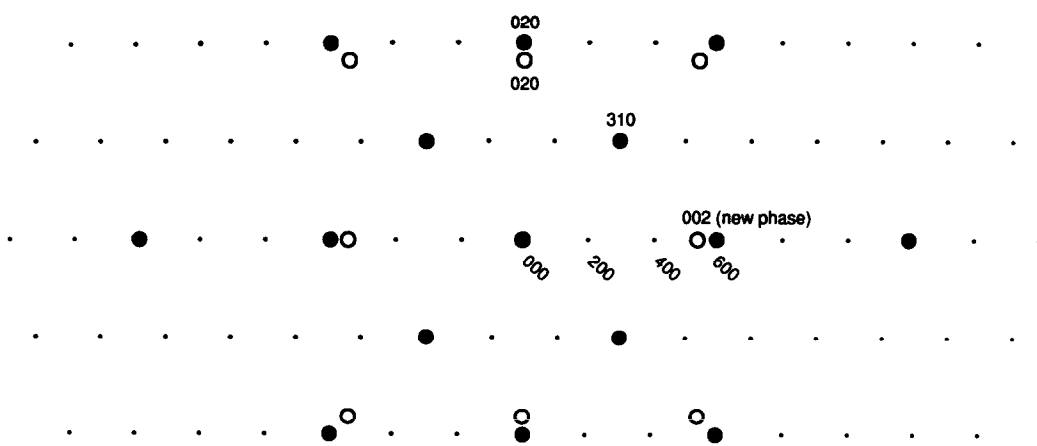
FIG. 5. A high-resolution image of $(V_{0.7}Mo_{0.3})_2O_5$. (a) At the beginning of observation. The undecomposed region is marked A. B marks a decomposed region. C marks a decomposed island in an undecomposed region. The region between them is in an intermediate stage. (b) After 20 min irradiation.

as Fig. 5a shows a region of a crystal of $(V_{0.7}Mo_{0.3})_2O_5$ that has already substantially decomposed; only a few regions such as that marked as A are essentially pristine. The white spots in the A region correspond to

the channels in the structure as illustrated in Fig. 1b. A completely reacted surface region is marked B, while a completely reacted island in the interior is labeled C. Most of the remainder of the crystal is in interme-
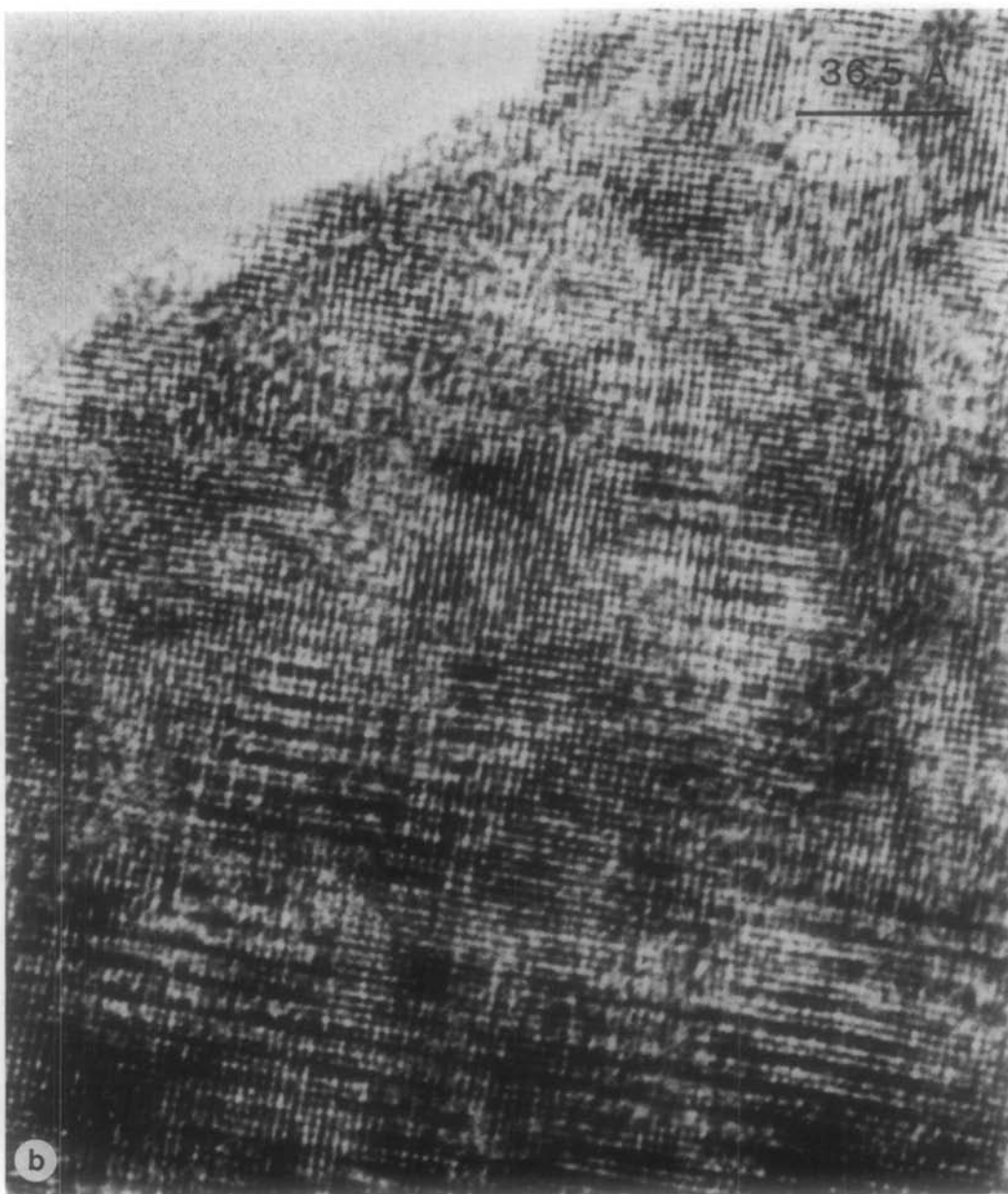
FIG. 5—*Continued*

diate stages of decomposition. Note the region just below the fully reduced surface layer that is characterized by double rows of white spots. This image is characteristic of much of the area of both Figs. 5a and 5b.

The latter was taken of an adjacent region 20 min later. It is apparent that, although the structure of the final product is the same in both these two *in-situ* reductions, the intermediate stages are clearly different. The in-
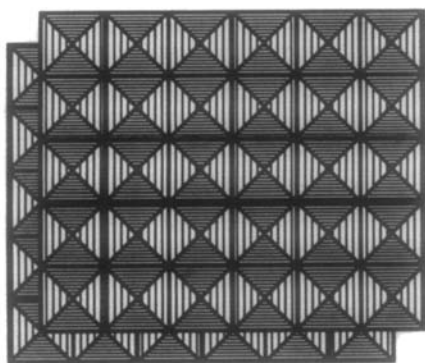
NaCl structure [100]

FIG. 6. The model of the NaCl-type structure is the [0 0 1] projection.

termediates from the more reduced phase appear to have a greater longevity in the beam. The final product is extremely disordered as before.

The image of the intermediate phase is clearly exhibited near the top center of Fig. 5a and in many regions of 5b. It is characterized by double columns of white spots that ultimately have essentially the same spacing as the square net of the final structure. However, in this structural image every third column, compared to the final product, is virtually missing. It has not been possible to

identify the intermediates from the numerous possibilities.

The Identity of the Final Product in the Two Overall In-Situ Reactions

Both V_2MoO_8 and $(V_{0.7}Mo_{0.3})_2O_5$ decompose, during imaging in the beam of a high-resolution electron microscope, to the same final product. We assemble here the observations and arguments that the final products are VO and MoO_x, where x may be zero.

The qualitative presence of oxygen in the final product is confirmed both by EDX and EELS analysis. Conditions do not permit obtaining a quantitative analysis in this case.

As shown above, the final image is compatible with an f.c.c. structure in which all the octahedral sites are filled with oxygen, in other words the NaCl-type structure (see Fig. 6). Such a phase is reasonable if the shear processes that convert the structure of V_2MoO_8 to $(V_{0.7}Mo_{0.3})_2O_5$ were continued until the entire structure consisted of octahedra sharing all edges. The orientational and dimensional relationships are entirely consistent with this model in both cases. That the final structure is NaCl-type is further supported by comparing the diffraction patterns observed with those calculated for NaCl-, ZnS-, and TiO$_2$-type. Figure 7 shows

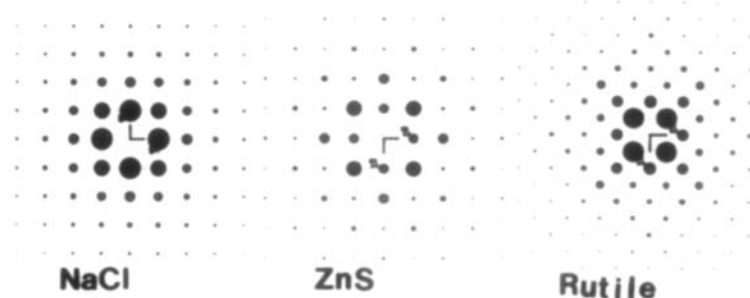

NaCl   **ZnS**   **Rutile**

FIG. 7. The calculated kinetimatic diffraction patterns of the NaCl-type, ZnS-type, and rutile-type structures.
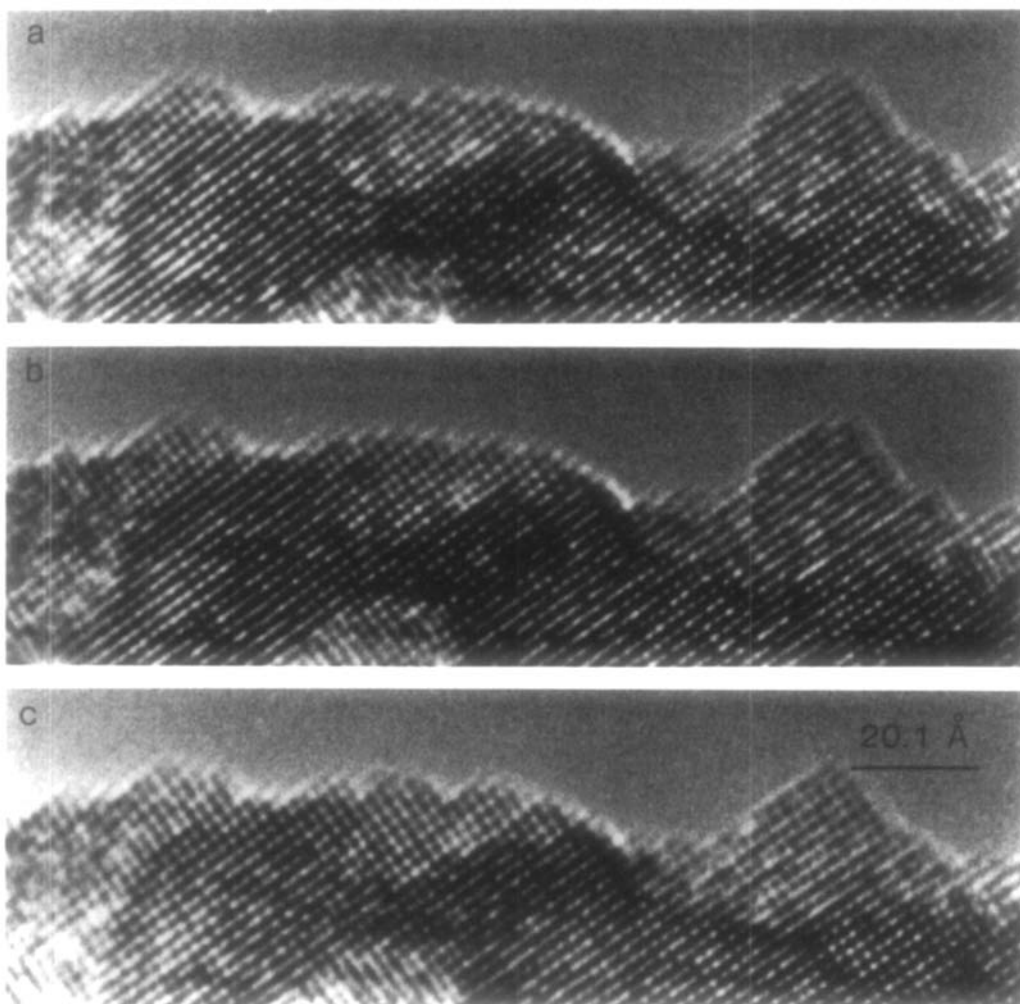
FIG. 8. A series of surface profile image showing the dynamic process of the formation of the product phase on the surface edge.

the calculated kinematic, electron diffraction patterns of these three structures. Consider the intensities of the innermost spots of the calculated patterns with the final product patterns from Figs. 2 and 4. The intensities and orientation of these four spots are consistent only with those of the NaCl-type.

NaCl-type VO is well known but MoO has not been established. Although mixed higher oxides are not unlikely, a mixed mon-

oxide with more than a trace of Mo would not be expected, therefore, it is most likely that the final f.c.c. compound is VO and that the Mo has been expelled and has collected on the surface or within the crystal as a molybdenum oxide or as molybdenum metal. Figures 3b and 5b show the crystal in an advanced state of decomposition, and in each case there are dark regions in which the square net of the f.c.c. phase is very weak or absent. It is supposed that the ex-

pelled molybdenum is concentrated in these regions.

Evidence of Atomic Surface Transport on the VO Decomposition Product

Figure 8 shows a sequence of three $\langle 1\ 0\ 0 \rangle$ surface-profile images recorded during an interval of about 30 min. Small but definite changes can be observed, and in this instance, a development of $\{1\ 0\ 0\}$ faces is perceived. Note, for example, the perfection and extension of the planar $\{1\ 0\ 0\}$ surface near the right side of the figure. Faceting along $\{1\ 0\ 0\}$ is clearly increasing in the region of the central bulge in the figure. A point to be made is that there is no profound reconstruction of the surface during the decomposition.

Conclusions

The *in-situ,* electron-beam-induced decomposition of V_2MoO_8 and $(V_{0.7}Mo_{0.3})_2O_5$ has been followed at near-atomic resolution. HREM techniques including electron diffraction and image simulation were used to establish the structures. EDX and EELS were used for chemical analysis in the study. The final decomposition product in both

cases was found to be oriented NaCl-type VO with a distributed residue incorporating the excess molybdenum. No ordered intermediate phase was observed in the reaction involving V_2MoO_8, however, there was a persistent ordered intermediate during the decomposition of $(V_{0.7}Mo_{0.3})_2O_5$, believed to be in the $[V_xMo_{(1-x)}]_2O_5$-type system.

No evidence was found for the oxidation of $(V_{0.7}Mo_{0.3})_2O_5$ to V_2MoO_8 in the electron beam, but rather reduction occurred in both instances.

Acknowledgment

References

1. Z. X. LIU, K. XIE, Y. Q. LI, AND Q. X. BAO, *J. Catal.* **119**, 249 (1988).
2. Z. C. KANG, Q. X. BAO, AND C. BOULESTEIX, *J. Solid State Chem.* **83**, 255 (1989).
3. H. A. EICK AND L. KIHLBORG, *Acta Chem. Scand.* **20**, 1658 (1966).
4. L. KIHLBORG, *Acta Chem. Scand.* **21**, 2495 (1967).
5. Z. C. KANG, C. CARANONIO, I. SINY, G. NIHOUL, AND C. BOULESTEIX, *J. Solid State Chem.* **87**, 308 (1990).